



## **Studying the effect of concentration of solutions on the properties of nickel oxide nanoparticles**

Shaymaa Mohammed FAYYADH<sup>1</sup>, Maha M. IBRAHİM<sup>2</sup> & Abeer Ibrahim ASHAWİ<sup>3</sup>

**Keywords**  
nickel oxide  
nanofilms, spin  
coating method,  
copper doping,  
optical properties.

### **Abstract**

In this study, copper doping concentrations of 0.02 and 0.04 were employed to create (NiO) films, which were then subjected to optical and structural tests, including X-ray diffraction, atomic force microscopy, and absorbance, reflectivity, and energy gap. The higher doping ratio resulted in a smaller value for the granular size by (62nm), whereas the pure films gave a granular size of (118nm), and this result agreed with the results of the XRD. The doping ratios did not affect the phase of the prepared films, but they did affect both the granular size and the specific surface area. The range of particle sizes used for the AFM analysis. According to the findings of the eye examinations, the absorbance and reflectivity increased with the amount of doping while the transmittance decreased. The membrane had an energy gap of 1.65 eV during the time when the pure membrane had an energy gap of 0.04Cu, but the energy gap shrinks as the amount of cu in the thin film grows (1.85 eV).

### **Article History**

Received  
7 Mar, 2023  
Accepted  
23 Jun, 2023

## **1. Introduction**

Thin films, which provide better physical properties of materials than those of those materials in their natural form, are one of the most significant technologies that have contributed to the development of semiconductors and their applications. [1], As a result of atoms or molecules condensing on a substrate (solid base), constructed of glass, silicon, or aluminum, depending on the nature of the study, a thin film is formed up of one or more layers of material atoms that are only one micrometer or several nanometers thick. Due to the impact of surfaces on the physicochemical properties of the membranes and the neglect of these surfaces, membranes have physical and chemical properties that are different from those of the materials that make up their constituent parts.

<sup>1</sup> Corresponding Author. ORCID: 0000-0003-1565-3170. University of Sfax, Faculty of Science of Sfax, Laboratory of Applied Physic, Tunisia, shymafaydh@tu.edu.iq

<sup>2</sup> ORCID: 0000-0003-4336-5205. Department Of Physics, College Of Science, Tikrit University, Iraq, Maha.ibrahim@tu.edu.iq

<sup>3</sup> ORCID: 0000-0003-3776-6715. College of Education for Basic Sciences, Tikrit University, Iraq, Abeer.ibraheem@tu.edu.iq

Due to the variety of applications for these layers, different film preparation methods are used. Thin films can be prepared using either a physical process or a chemical method. The choice of one method over another depends on a number of variables, the most crucial of which are the kind of material employed, the application area for the layer that was prepared, and the cost of preparation. As there are some procedures that are suitable for materials and not suitable for other materials, and since some of them are simple to use and others are complex, the techniques that are characterized by low economic cost have drawn a lot of attention [3]. The rotary coating method was used in this study because it requires the substrate to be rotated at a high speed while the gel solution is poured on it drop by drop. As a result, the sedimentation material is distributed across the substrate by the action of centrifugal force, and the layer thickness can be changed by adjusting the rotation and acceleration. The major purpose of this treatment is to eliminate crystalline flaws and hence enhance the properties of the membranes in terms of permeability and crystallinity [4,5]. This treatment is also dependent on the viscosity of the gel solution, where the solvent evaporates extremely quickly.

## 2. Experimental Part

### 2.1. Preparation of solutions

#### 2.1.1. Prepare pure sample solution

In order to create (NiO) films, aqueous nickel nitrate ( $\text{Ni}(\text{NO}_3)_2 \cdot 6\text{H}_2\text{O}$ ) with a molecular weight of ( $M = 290.8 \text{ g/mol}$ ) was used. The weights of nickel nitrate needed to be combined with ( $V = 15 \text{ ml}$ ) of distilled water to create a solution with a concentration of ( $C = 0.3 \text{ mol/l}$ ) can be determined using the relationship (1): [6]

$$m = C.M.V \text{-----} \quad (1)$$

whereas-:

m : the weight to be used

C : molar concentration in mol/gm

M: The molecular weight of the substance used in gm/mol

#### 2.1.2. Preparation of impure samples solution

To inoculate nickel oxide with copper, two molar ratios of (0.02,0.04) mol of the inoculation solution (quantitative copper nitrate) were used for all molar concentrations of the basic ( $\text{Ni}(\text{NO}_3)_2 \cdot 6\text{H}_2\text{O}$ ) with a volume of ( $V_s = 15 \text{ ml}$ ) as in the equation (2).[7]

$$(V_s2/V_s1) \times 100 = W \text{-----} \quad (2)$$

$V_s1$ : volume of the base solution (aqueous nickel nitrate solution).

$V_s2$ : the volume of the inoculation solution (the solution in which the aqueous copper nitrate is dissolved).

W: volumetric percentage of inoculum.

Note that the molecular weight of aqueous copper nitrate is (241.45 gm/mol).

## 2.2. Prepare the glass bases

We used glass substrates of the type (0004-0302-CITOPPLUS- REF) with dimensions (75 mm×25). These substrates were cleaned to get rid of sediment in several stages, namely:

- By immersing the glass substrates in chloric acid (HCl) and then in ethanol solution, then cleaning them with distilled water to ensure the quality of cleaning .
- The substrates were placed in ethanol with the chemical formula (C<sub>2</sub>H<sub>5</sub>OH) for 10min, then extracted from the solution and dried at a temperature of 60°C for 10min.
- Then it was placed in acetone with the chemical formula (C<sub>3</sub>H<sub>6</sub>O) for 10 minutes, then it was extracted from the solution and dried at a temperature of 60°C for 10 minutes.

After all these steps, the models are ready for painting.

### 2-3 Rotational coating process steps (Sol-Gel)

The process of deposition on the films is carried out using the rotary coating method, following the following steps:

- After leaving the prepared solution for 24h, we filter the solution using filter paper to ensure that the solution is free of any impurities and also to ensure the homogeneity of the solution.
- We put the glass substrates after cleaning and put them on the base of the device and use a micro-burette to withdraw an amount of 50µml and drip onto the substrate and then operate the device at a speed of (3000 rpm) for 30sec and then turn off the device and repeat the process again after several minutes on the same slide .
- the samples were dried at a temperature of 100°C for a period of (10min), after which they were left to until room temperature was reached.

## 3. Examinations

### 3.1. The test of X-Ray-Diffraction

Using an X-ray diffraction machine from Shimadzu Corporation. The interstitial distances values for atomic levels (d) were obtained for each sample using equation (3) [8].

$$n\lambda = 2d \sin\theta \quad \text{----- (3)}$$

For the purpose of calculating the particle size of the formed material, we use equation (4) [9].

$$D = \frac{k\lambda}{B \cos\theta} \quad \text{----- (4)}$$

D :- particle size.

λ :- X-ray wavelength.

K :- Constant form factor.

$\beta$  :- width middle beck

$\theta$  :- Brack angle

Through equation (5) we can calculate the surface area (S) [10]:-

$$D = \frac{6}{S \rho} \quad \text{----- ( 5)}$$

D: particle size, nm

S: Specific surface area (m<sup>2</sup> /gm)

$\rho$ : surface area density

### 3.2. Atomic force microscopy (AFM) examination

The atomic force microscope (AA 3000 SPM) was used in this research to study the surface topography of the samples (particle size and surface roughness rate).

### 3.3. Optical examinations

The UV-1800 (UV Visible Spectrophotometer) spectrometer was used to produce optical measurements for the wavelength range (200-1100) nm in order to conduct visual examinations. in the reference window, the fundamental rule. For the above-mentioned range of wavelengths, optical measurements included measuring transmittance and absorbance. Using the relationships (6), (7), (8), and (9), we will calculate the optical properties of transmittance, reflectivity, suppression coefficient, absorption coefficient, and energy separation. [11,12,13,14]

$$T = e^{-\alpha d} \quad \text{----- (6)}$$

$$A (\text{cm}^{-1}) = 1/d \ln \left( \frac{100}{T(\%)} \right) \quad \text{----- (7)}$$

$$K = \frac{\alpha \Delta}{4\pi} \quad \text{----- (8)}$$

$$(\alpha h\nu)^2 = B (h\nu - E_g) \quad \text{----- (9)}$$

B is a constant

E<sub>g</sub>: energy interval and its unit (eV)

h $\nu$  : photon energy and its units (eV)

## 4. Results and discussion

### 4.1. Effect of copper doping on particle size and specific surface area

The (XRD) inspection of the produced films revealed directions (111), (200), and (220) at angles (38.2, 43, and 67.1), respectively, and they were noticeably different in appearance between the inlaid and untreated films, as shown in Figure 1. All of the prepared films gave off a polycrystalline structure of the cubic type as shown in the international card ASTM (card 04-0835), and table (1) demonstrates that the percentage of inoculation affected the particle size even though the phase

of all the prepared films was unaffected by the inoculation condition. Increases in the proportion of copper inoculation also increased the surface area of the membranes by causing a reduction in particle size. In line with [15,16,17,18]

**Figure 1.** X-ray diffraction of the doped and undoped films

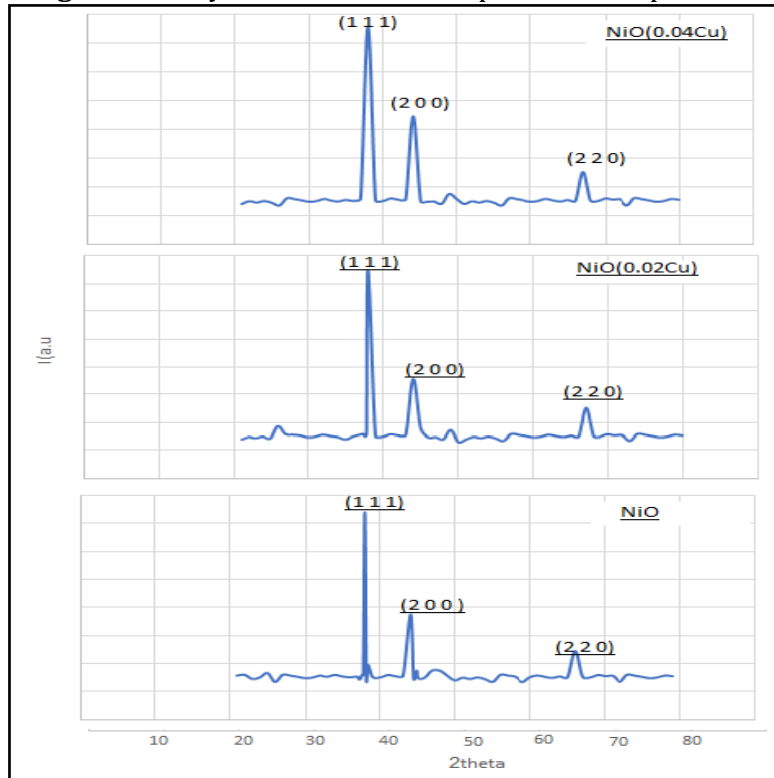


**Table 1.** Shows the particle size and surface area of the thin films

Models	S (m <sup>2</sup> /mg)	D (nm)
NiO	7.6	118
NiO(0.02Cu)	12.8	70
NiO(0.04Cu)	14.5	62

#### 4.2. The effect of copper doping on the results of atomic force microscopy

Figures (2), (3), and (4) show AFM pictures made with NiO, NiO(0.02Cu), and NiO(0.04Cu), respectively. In these images, we can see how the distribution of particle sizes on the film surfaces varies for different percentages. The average particle size falls as the inoculation percentage increases, but the surface roughness rate is different since it increases as the inoculation percentage increases, whereas the non-copper-doped films give an average value of (321nm).

**Figure 2.** Shows AFM images of a thin film (NiO).

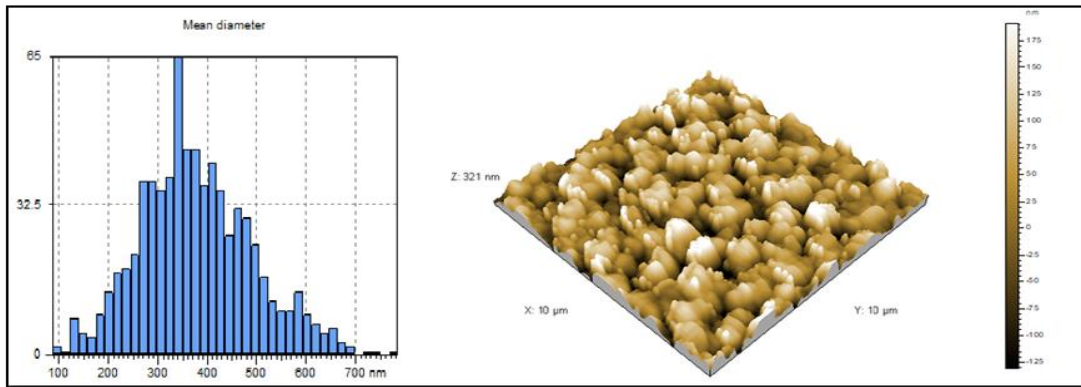


**Figure 3.** Shows the AFM images of thin film NiO (0.02Cu).

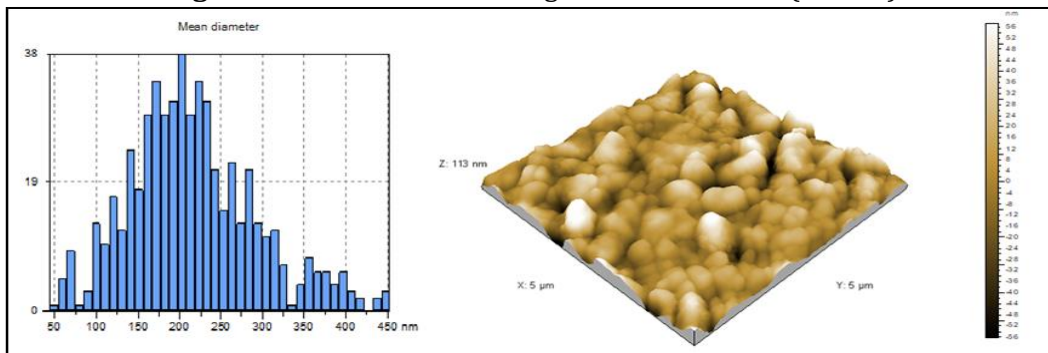


**Figure 4.** Shows AFM images of thin film NiO (0.04Cu)

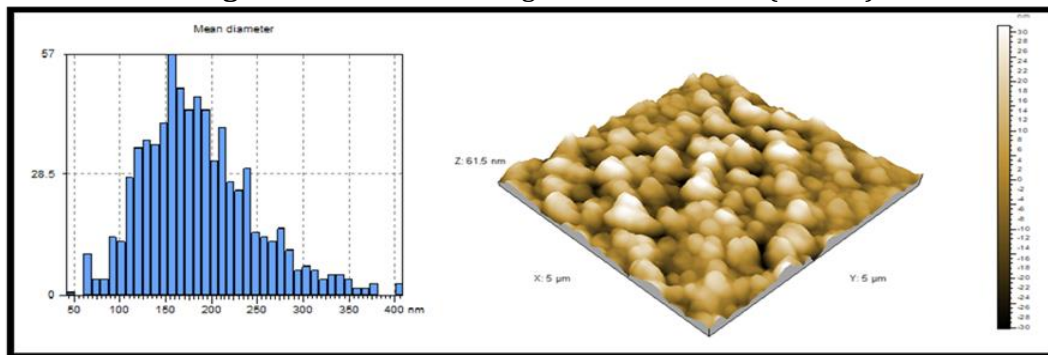


**Table 2.** Shows the average particle size and surface roughness of the films

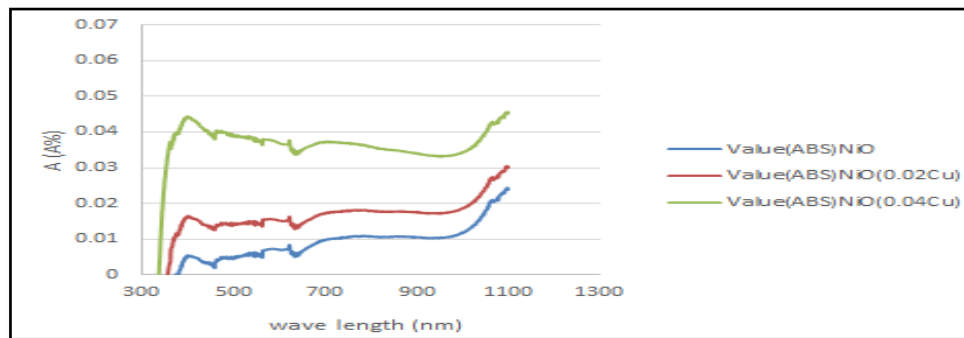
Models	Average Grain Size (nm)	Roughness Average (nm)
NiO	330	321
NiO(0.02Cu)	200	113
NiO(0.04Cu)	150	615

### 4.3. Effect of doping on optical properties

#### 4.3.1. Absorbance

The maximum absorbance values were for the doped films with larger doping ratios, and the lowest values were for the undoped films, as shown in Figure (5). This is due to the small grain sizes of the doping ratio (0.04Cu) and the high granular sizes of the NiO, which increases the surface area of the doped films and raises absorbance. These films received less photon energy than undoped films, which had smaller surfaces and so produced somewhat lower absorption results. The area caused the prepared films to behave zigzag, but when the near infrared region approached, the absorbance levels started to increase once more.

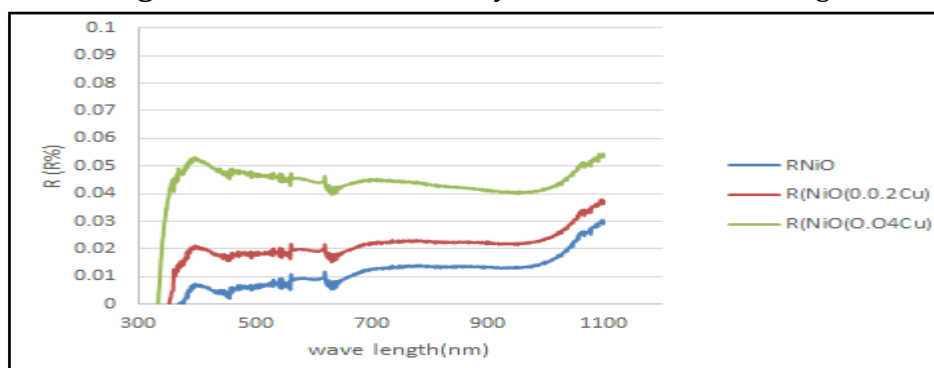
Figure 5. Shows the absorbance as a function of wavelength



#### 4.3.2. Reflectivity

Figure (6) depicts the relationship between reflectivity and wavelength. The behavior of the reflectivity is comparable to that of the absorbance with respect to the incident photon's wavelength and the produced films' copper doping percentages.

Figure 6. Shows the reflectivity as a function of wavelength

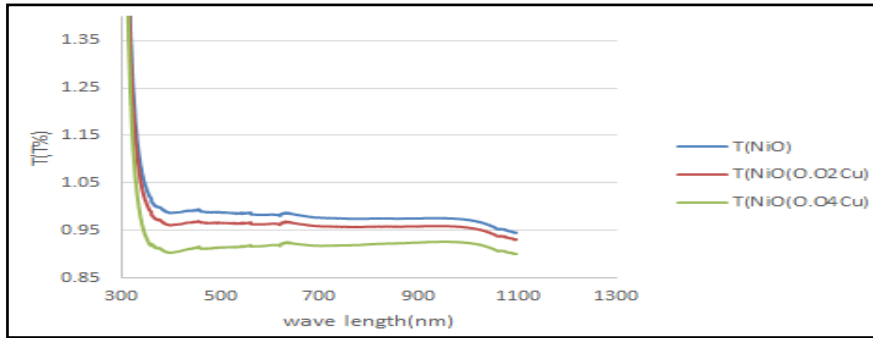


#### 4.3.3. Transmittance

Figure (7) shows the relationship between the wavelength of the incoming photon and the transmittance of the prepared membranes. We note that the highest transmittance values were in the ultraviolet region, or before the absorption edge, but that there was a decline in transmittance values after the absorption edge to support these values for wavelengths between (400nm) and (800nm) (1100nm) In terms of the impact of copper doping, the (0.02Cu) and (0.04Cu) films had the

lowest values of transmittance along the wavelength path in contrast to the (NiO) film, which had the highest values.

**Figure 7.** shows the transmittance as a function of wavelength



#### 4.4. Effect of copper doping on the energy gap

Figures (8), (9) and (10) show that, in contrast to films doped with lower percentages, those doped with higher percentages of copper have a positive relationship between the values of the allowed direct transmission energy and the energy of the incident photon, whereas the values of the undoped films had a more stable relationship with energy values. We note that the allowed direct transition energy values increased very quickly after increasing the photon energy values above the energy gap values, and from Table (3) we find that by increasing the doping values, the gap values decreased energy compared to the undoped films. These two relationships for the doped and undoped films showed similar behavior.

**Figure 8.** Direct allowable transition energy relation to photon energy (NiO).

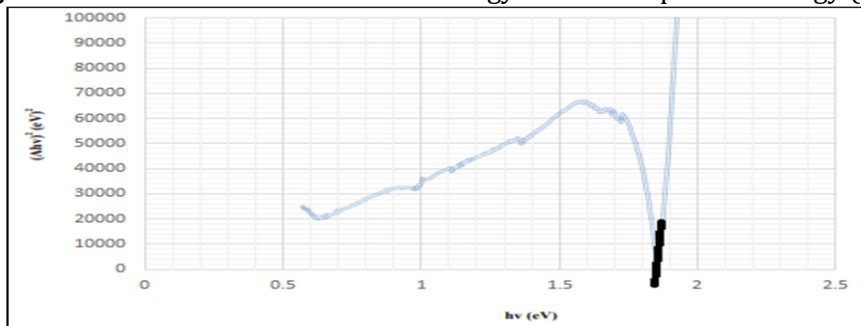


**Figure 9.** Direct allowable transition energy relation to photon energy (0.02Cu)(NiO).

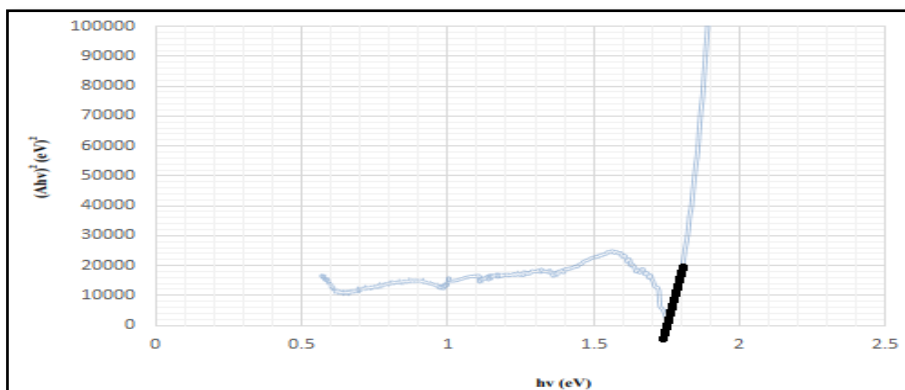


**Figure 10.** Direct allowable transition energy relation to photon energy(0.04Cu)(NiO).

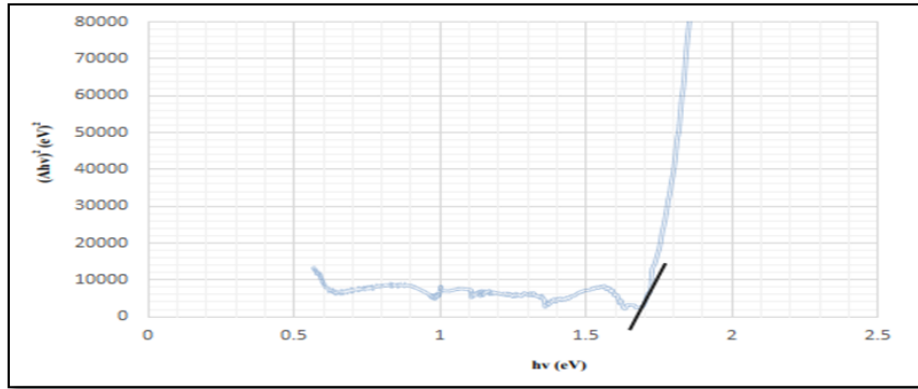


**Table 3.** Shows the energy gap values

Models	Eg(e V )
NiO	1.85
NiO(0.02Cu)	1.75
NiO(0.04Cu)	1.67

## 5. Conclusions

- The particle size of the produced films reduces when the inoculation rates are increased, increasing the specific surface area.
- For all membranes, the absorption values rise in the visible alkaline wavelength range and the region of the near infrared spectrum.
- We see a marked improvement in the energy gap values as the doping rates are increased; the energy gap of NiO films was (1.67 eV) when doped with a ratio of (0.04Cu), whereas it was (1.85eV).

## References

- [1] Abubakar, D., Ahmed, N. M., & Mahmud, S. (2019). The study on the effect of wet and dry oxidation of nickel thin film on sensitivity of EGFET based pH sensor. In *Solid State Phenomena* (Vol. 290, pp. 199-207). Trans Tech Publications Ltd.
- [2] Wang, Y., Chen, M., Wang, C., Meng, X., Zhang, W., Chen, Z., & Crittenden, J. (2019). Electrochemical degradation of methylisothiazolinone by using Ti/SnO<sub>2</sub>-Sb<sub>2</sub>O<sub>3</sub>/α, β-PbO<sub>2</sub> electrode: Kinetics, energy efficiency, oxidation mechanism and degradation pathway. *Chemical Engineering Journal*, 374, 626-636.
- [3] Sabzevar, P. S., Bagheri–Mohagheghi, M. M., & Shirpay, A. (2022). The effect of rGO and chemical reduction under hydrazine on the structural, electrical and optical properties of nanostructured SnO<sub>2</sub>: F/rGO thin films. *Physica B: Condensed Matter*, 646, 414310.

- [4] Abu-Yaqoub, A. Y. S. (2012). Electrochromic Properties of Sol-gel NiO-based films (Doctoral dissertation).
- [5] Dastan, D., Jafari, A., Marszalek, T., Mohammed, M. K., Tao, L., Shi, Z., ... & Ansari, L. (2023). Influence of heat treatment on H<sub>2</sub>S gas sensing features of NiO thin films deposited via thermal evaporation technique. *Materials Science in Semiconductor Processing*, 154, 107232.
- [6] Harvey, D. (2011). *Analytical Chemistry 2.0—an open-access digital textbook. Analytical and bioanalytical chemistry*, 399(1), 149-152.
- [7] Christian, G. D., Dasgupta, P. K., & Schug, K. A. (2013). *Analytical chemistry*. John Wiley & Sons.
- [8] Razzoqi, R. N., Mahmood, L. A., Ahmed, M. S., & Fayyadh, S. M. (2012). Influence of the chemical composition and pressure of the compressing on some physical and mechanical properties of ceramic matrix composite. *International Review of Mechanical Engineering*, 6(3).
- [9] Aljuraid, N. I. (2011). Mössbauer Effect Study of Some Nano metric Samples Containing Iron.
- [10] Mascolo, M. C., Pei, Y., & Ring, T. A. (2013). Room temperature co-precipitation synthesis of magnetite nanoparticles in a large pH window with different bases. *Materials*, 6(12), 5549-5567.
- [11] Mascolo, Maria Cristina; Pei, Yongbing; RING, Terry A. Room temperature co-precipitation synthesis of magnetite nanoparticles in a large pH window with different bases. *Materials*, 2013, 6.12: 5549-5567.
- [12] Boubrik, N. (2013). Comparaison des effets antireflets du SnO<sub>2</sub> et ZnO utilisés comme couches antireflet sur les propriétés de la cellule solaire à homo-jonction (Doctoral dissertation, Université Mouloud Mammeri).
- [13] Al-Alawy, A. F., Al-Abodi, E. E., & Kadhim, R. M. (2018). Synthesis and characterization of magnetic iron oxide nanoparticles by co-precipitation method at different conditions. *Journal of Engineering*, 24(10), 60-72.
- [14] Sharma, P., Sharma, N., Sharda, S., Katyal, S. C., & Sharma, V. (2016). Recent developments on the optical properties of thin films of chalcogenide glasses. *Progress in Solid State Chemistry*, 44(4), 131-141.
- [15] Chen, H. L., Lu, Y. M., & Hwang, W. S. (2006). Thickness dependence of electrical and optical properties of sputtered nickel oxide films. *Thin Solid Films*, 498(1-2), 266-270.
- [16] Ail, A. H., & Kadhim, R. R. (2015). Effect of copper doping on the some physical properties of NiO thin films prepared by chemical spray pyrolysis. *International Journal of Application or Innovation in Engineering & Management*, 4, 2319-4847.
- [17] Hamdi, A. A., & Ismail, O. D. (2021). Some of the Study of the Physical Properties of the Membranes Binary Tin Oxide [SnO<sub>2</sub> sub. 2] Pure and Tinged with Nickel Ni at Different Rates Distortion. *NeuroQuantology*, 19(10), 95-100.

- [18] De Los Santos Valladares, L., Ionescu, A., Holmes, S., Barnes, C. H., Bustamante Domínguez, A., Avalos Quispe, O., ... & Majima, Y. (2014). Characterization of Ni thin films following thermal oxidation in air. *Journal of Vacuum Science & Technology B, Nanotechnology and Microelectronics: Materials, Processing, Measurement, and Phenomena*, 32(5), 051808.
- [19] Singh, I., Dey, S., Santra, S., Landfester, K., Muñoz-Espí, R., & Chandra, A. (2018). Cerium-doped copper (II) oxide hollow nanostructures as efficient and tunable sensors for volatile organic compounds. *ACS omega*, 3(5), 5029-5037.

© Copyright of Journal of Current Research on Engineering, Science and Technology (JoCREST) is the property of Strategic Research Academy and its content may not be copied or emailed to multiple sites or posted to a listserv without the copyright holder's express written permission. However, users may print, download, or email articles for individual use.